NURail2012-MTU-R01

Austempered Ductile Iron (ADI) For Railroad Wheels

By

Karl Warsinski
Graduate Research Assistant
Department of Materials Science and Engineering
Michigan Technological University
E-mail: kcwarsin@mtu.edu

and

Paul G. Sanders, Ph.D.
Associate Professor
Department of Materials Science and Engineering
Michigan Technological University
E-mail: sanders@mtu.edu

Grant Number: DTRT12-G-UTC18

DISCLAIMER

Funding for this research was provided by the NURail Center, University of Illinois at Urbana - Champaign under Grant No. DTRT12-G-UTC18 of the U.S. Department of Transportation, Office of the Assistant Secretary for Research & Technology (OST-R), University Transportation Centers Program. The contents of this report reflect the views of the authors, who are responsible for the facts and the accuracy of the information presented herein. This document is disseminated under the sponsorship of the U.S. Department of Transportation's University Transportation Centers Program, in the interest of information exchange. The U.S. Government assumes no liability for the contents or use thereof.

TECHNICAL SUMMARY

NURail2012-MRU-R01 Final Report January 30, 2017

Title

Austempered Ductile Iron for Railroad Wheels

Introduction

The purpose of this project is to investigate the potential for austempered ductile iron (ADI) to be used as an alternative material for the production of rail wheels, which are currently cast or forged steel which is commonly heat treated. ADI has several potential advantages over steel, including lower production costs (20% savings for a typical component) while maintaining strength-to-weight ratios equivalent to heat treated steels, and microstructure-based noise damping[1]. Preliminary work in Europe also suggests that ADI wheels may reduce both wheel and rail wear, increasing equipment and infrastructure life [2]. There are concerns about the fatigue cracking of ADI wheels due to localized strain-induced transformation of austenite to martensite. However, appropriate wheel design adjustments can be made to address this [3]. In order to take advantage of these characteristics, it is necessary to first characterize ADI's microstructural stability with respect to elevated temperatures that result from on-tread braking. The key microstructural component in ADI is ausferrite, which is a combination of the stable room temperature phase (ferrite) with the meta-stable higher temperature phase (austenite). Because of the presence of the meta-stable austenite phase, ADI is susceptible to changes in properties at elevated temperatures. Heat-treated steel wheels currently in use are also susceptible to changes in structure and properties as a result of overheating. The primary purpose of this project is to identify the conditions necessary for the decomposition of the ausferrite microstructure and compare them with rail wheel service conditions. Then, methods for stabilizing the ausferrite structure thermodynamically and kinetically are explored.

It should also be noted that the minimum mechanical properties of the standard ADI grades do not align well with the AAR standards for rail wheel properties. Standard ADI is permitted to have lower elongation in all grades than is permitted for rail wheels [4], [5]. Grades 3-5 meet the strength requirements for rail wheels, but as the strength increases the minimum elongation falls farther from the value required by the AAR standard.

Approach and Methodology

The approach used in this research was to characterize the thermal service conditions of rail wheels and correlate them to a kinetic model of the thermally induced breakdown of microstructure of austempered ductile iron. There were three main tasks:

- The first task was to characterize the thermal conditions experienced by rail wheels in service, both via literature search and through direct measurement of wheel tread temperatures on a class III railroad. The measured temperatures and heating rates were too low to pose a concern, so values found in the literature representing more severe operating conditions were used for further comparison.
- Second, Differential Scanning Calorimetry (DSC) was used to determine the activation energy for the transformation in question in commercially produced ADI. This value can then be used to model the time required at a given temperature before the microstructure (and therefore properties) of the material will change. This particular metric was chosen because the effective (measured) activation energy can be compared across alloy variations, even if the transformation mechanisms vary. Scans at three heating rates were performed for each sample material. The transformation peak onset temperatures were then used to determine the activation energy for each grade.
- The third stage was an effort to determine the effects of alloying elements on the stability of ADI. Thermodynamic modeling was used to plot phase diagrams illustrating the effects of various common alloying elements on the thermodynamic stability of austenite. These plots show changes in the driving force for austenite decomposition caused by common alloying elements. Additional alloy variations were chosen based on their reported effects on the kinetics of carbon diffusion.

Five test alloys were produced in the Michigan Tech Foundry. The alloy compositions were chosen based on commercially produced ADI, and each heat varied one of the chosen elements. Test bars from each composition were then heat treated to match the heat treatments from the initial assessment of commercially produced ADI (Task 2). A more detailed description the study methods and outcomes has been provided in the following Technical Report.

Findings

Since the performance in high temperatures is one of the critical capacities of railroad wheels, an attempt was made to measure the in-service wheel temperatures during a heavy braking application of a unit train operation. However, due to slow speeds involved, the measured temperatures did not exceed 115°C. The literature shows that it is common for rail wheels to reach 300°C, and simulations indicate that brake system failures (stuck brakes, loss of dynamic braking, etc.) could cause wheel tread temperatures to exceed 550°C [6]. The analysis of ADI's performance in elevated temperatures were done with these thresholds in mind.

Differential scanning calorimetry has been shown to be a useful technique for comparing the kinetics of austenite decomposition in ADI. At a constant heating rate of 10 K/min (comparable to that observed in service on a class III railroad), the onset of austenite decomposition occurs at temperatures approaching the thermal limits for the steels currently used for rail wheels, in the range 450-500°C. This indicates that ADI could handle normal service conditions, but could be compromised in an emergency condition. As is common in kinetically limited transformations, the transformation onset temperature increases with increasing heating rate.

The activation energies found in the commercial ADI samples range from 76 kJ/mol in Grade 1 down to 57 kJ/mol in Grade 5. Initial scans show an average value of 44 kJ/mol for Grade 3, but variability in that data set was very large, and additional scans are necessary before a conclusion can be drawn.

Thermodynamic and kinetic strategies for ADI stabilization have been selected based on modeling and

literature data. Alloying additions of nickel and cobalt are expected to provide thermodynamic stabilization, while the use of molybdenum to compete with iron carbide formation should provide a kinetic improvement. Initial results indicate that cobalt additions provide improved thermal stability, but more work is needed to fully characterize the effect.

Conclusions

Utilization of ADI the opportunity to reduce weight, noise, and cost with improved wear performance. These potential benefits warrant continued investigation of its use in the wheels of both passenger and freight rail rolling stock. The key challenge is the stability of the ausferrite microstructure (formed during austempering) at elevated service temperatures (e.g. braking). In this work, the onset of austenite decomposition occurs at temperatures comparable to the thermal limits for steel wheels. Typical service in North America results in wheel temperatures up to ~315°C, but of course more extreme conditions must be accounted for[8], [9].Based on preliminary stability results, it appears that the lower strength ADI grades (1 and 2) are more thermally stable than their stronger counterparts. However, these grades still cannot meet the strength and elongation requirements for rail wheels as set out in AAR M-107/M-208. Utilizing thermodynamic modeling to inform the production of new ADI compositions, cobalt has been identified as potentially improving the thermal stability of the ausferrite matrix.

Recommendations

Further exploration of ADI stabilization strategies will be necessary to achieve a balance between thermal stability and mechanical properties that is suited to rail wheel applications. Despite some earlier research, the upper boundary of wheel temperatures is also somewhat unclear, both for freight and passenger applications. Therefore, a model for the service temperature histories of railroad wheels should be developed to better understand the effects of heating cycles on wheel life, both for existing steel wheels and for prospective wheel materials like ADI.

While beyond the scope of this project, it is also recognized that it will be necessary to develop a thorough understanding of the residual stress patterns resulting from austempering of ductile iron in rail wheels, as well as the rolling contact fatigue behavior of any alloy developed as a result of this research.

Publications (Appendix A)

Warsinski, K., Lautala, P. and Sanders, P. (2014). *Austempered Ductile Iron Performance at Rail Wheel Operating Conditions*. Proceedings of the 2014 ASME Joint Rail Conference. April 2-4, Colorado Springs, Colorado.

Warsinski, K., Lautala, P. and Sanders, P. (2016). Application of Differential Scanning Calorimetry for the Determination of ADI Service Temperature Limits, World Conference on Austempered Ductile Iron Conference Proceedings, October 27-28, Atlanta, Georgia.

Primary Contact and Principal Investigator
Paul Sanders, Ph.D.
Associate Professor
Department of Materials Science and Engineering
Michigan Technological University
1400 Townsend Drive, Houghton MI 49931
Email: sanders@mtu.edu

Other Faculty and Students Involved
Karl Warsinski
Graduate Research Assistant
Department of Materials Science and Engineering
Michigan Technological University
Email: kcwarsin@mtu.edu

NURail Center
217-244-4444
nurail@illinois.edu
http://www.nurailcenter.org/

Pasi Lautala, Ph.D., P.E.
Michigan Technological University
Rail Transportation Program
1400 Townsend Drive
Houghton, MI 49931
ptlautal@mtu.edu

TABLE OF CONTENTS

LIST OF FIGURES

Figure Page

SECTION 1 INTRODUCTION

1.1 *Background and Motivation*

Currently, the Association of American Railroads (AAR) requires the use of carbon steel wheels for rail service [5]. The steel used is a medium carbon steel with less than 1% manganese and minimal amounts of sulfur, phosphorous, and silicon. The wheels may be cast or forged, but must be heat treated if used for "severe service conditions". Since railcars are regularly transferred between lines and used for various cargo, this requirement applies fairly broadly. Rail wheels are safety critical components, so the qualification requirements for manufacturers are significant, and industry changes to wheel designs and materials take a great deal of time.

The primary cause of failure of rail wheels is rolling contact fatigue, which can lead to cracking or spalling of the tread surface. The residual stresses from heat treatment of steel wheels must be carefully managed to avoid a residual tensile stress along the tread, which would promote fatigue cracking. However, the manufacturing process isn't the only factor. The tread of the wheel is used as the rolling contact surface with the rail, but also serves the function of a brake disc, with the braking pad applied directly to the wheel tread. This results in frictional heating, which can alter the residual stress patterns within the wheel. If thermal cycling sets up a tensile component on the tread surface while in service the wheel can break, which may be enough to derail a train. If the tread reaches austenitizing temperatures, it is possible to form brittle martensite on cooling, which is more prone to cracking and spalling.

Steel suits the rail wheel application due to its high strength and durability, but it does have drawbacks. Steel is difficult to cast, making it an expensive alloy to use. Forging is more expensive than casting, since the steel must first be made and cast into billets, and then additional energy is required to produce the final shape (though this does have the benefit of added strength). Steel rolling on steel causes significant wear on both the wheels (which must be periodically replaced) and on the rail (which can be re-ground several times before replacement).

Austempered ductile iron (ADI) is still relatively new as cast iron goes (first commercialized in the early 1970s), but has significant potential for cost, wear, weight and noise reduction when compared with steel. These benefits make it worth investigating as an alternative to cast steel for railroad wheels[2].

Ductile iron is functionally a metal-matrix composite, with small spheroidal nodules of graphite distributed within a ferrous matrix. As-cast ductile iron usually has a matrix that is a mixture of ferrite and pearlite, phases which are also commonly found in steels at room temperature. In ADI, the ferrous matrix is comprised of tiny needles of ferrite distributed in carbon-stabilized austenite. This structure is referred to as ausferrite, and is not generally found in steel. The austenite has higher strength than ferrite, without the brittleness associated with martensite. The fine ferrite needles also contribute to the iron's strength, because the phase boundaries impede dislocation movement necessary for deformation. While the graphite nodules are too soft to bear significant load themselves, their nodularity (a measure of roundness) makes them less prone to crack propagation than the flakes found in gray iron. The presence of distributed graphite provides the carbon saturation required for ausferrite formation, and also provides a vibration damping effect by breaking up resonance waves passing through the material.

Ausferrite is produced by heat treating high quality ductile iron. The heat treatment involves fully

austenitizing the matrix to homogenize the matrix carbon content. The iron is then rapidly quenched to avoid pearlite formation and then held at a temperature above the martensite start temperature long enough for ferrite to nucleate and grow. Carbon is rejected from the ferrite needles into the surrounding austenite, and the resulting supersaturation of carbon depresses the martensite transformation, stabilizing the austenite. The iron is cooled to room temperature when the austenite has been fully stabilized but before carbides have a chance to nucleate and relieve the supersaturation. This stabilization is kinetic in nature, rather than thermodynamic. Properly heat treated ADI will not form martensite even well below 0°C, but is still thermodynamically metastable. Exposure to high service temperatures can provide enough thermal energy for carbon diffusion, causing the carbon-enriched austenite to decompose by nucleating cementite (iron carbide), allowing the ferrite to resume growth. Any such phase transformation will result in changes in mechanical properties that may compromise the serviceability of the component [29]. It is also important to note that the nucleation location of the cementite is dependent upon the heat treatment parameters, most notably the austempering temperature. Forming a new phase requires overcoming an energy barrier, and the amount of energy required depends on the type of nucleation site. At higher temperatures, such as those used for Grade 1 ADI, there is more energy available for carbon diffusion, so carbide nucleation is more likely to occur at grain boundaries, where the existing surface energy offsets the energy required to produce a new surface. At lower austempering temperatures, as used for production of Grade 5 ADI, carbon diffusion is much slower, and carbide nucleation occurs within the existing austenite grains, allowing the surrounding grain to transform into ferrite. This nucleation must take advantage of dislocations and compositional variation, and requires a higher activation energy.

The bulk density of ADI is lower than steel because part of the volume is taken up by graphite, and yet the high strength of carbon-stabilized austenite leads to a bulk tensile strength comparable to steel. This high strength-to-weight ratio of ADI could be used to reduce rolling stock weight while retaining current axle loads, increasing the load carrying capacity of the rail car and reducing the energy demands to overcome resistances. In addition, the distributed graphite nodules offer a source of self-lubrication at the surface, which has been shown to decrease wear on both the wheels themselves and on steel rail [2]. This would reduce maintenance costs for both rolling stock wheels and rail infrastructure, although there is some indication that design adjustments may be needed to avoid fatigue cracking on the surface of the wheel tread [3].

The advantages of ADI seem clear, but the potential for thermally-induced transformation of the austenite, weakening the component, is a point of concern. Railroad wheels regularly undergo frictional heating as a result of on-tread braking [9]. This cyclic heating has to be taken into account during production of the current steel wheels, and naturally must be considered before ADI wheels can be put into service. The purpose of this study is to characterize the effects of heating on ADI, and to work towards development of alloy composition and heat treatment recommendations to produce ADI suitable for railroad wheels.

1.2 *Study Objectives*

This study had three objectives:

- An evaluation of service conditions by both literature review and direct measurement was conducted to form a frame of reference for what ADI wheels must withstand in service.
- The main focus of this study was to evaluate the kinetics of the austenite (γ) → ferrite (α) +

cementite (Fe_3C) transformation in austempered ductile iron. Thermal analysis was used to determine the activation energy for this transformation as a function of austempering temperature.

- Thermodynamic modeling was used to identify alloying elements that influence the driving force for austenite decomposition. Alloy variations were produced to determine the effects of these alloy additions on the transformation kinetics, in order to alloy improvements to ADI stability.

In addition, an electromagnetic sensor was designed to monitor the transformation response of ADI under isothermal conditions, in order to corroborate the kinetic measurements. The calibration and control software for this sensor is still under development.

SECTION 2 EVALUATION OF RAIL WHEEL SERVICE CONDITIONS

2.1 *Heating Rates – Direct Measurement*

There is relatively little directly measured data regarding wheel tread temperatures in railroad service available in the literature. The service environment is not particularly conducive to long-term sensor implementation on the wheel set, and wayside monitoring is generally focused on the bearing, rather than the wheel tread.

Early in this project, infrared sensors were mounted to the trucks of two iron ore cars at the Lake Superior and Ishpeming Railroad (LS&I) prior to an ore run with a 7.2-mile long 1.6% downgrade, and removed once the train stopped in the dockyard. The sensors were mounted to the front trucks of the first and eighth cars, and a radio transmitter was connected to the top of each car's ladder. The transmitters linked to a receiver in the second locomotive to record tread temperatures throughout the trip. The sampling frequency was 0.5 Hz, and the trip took approximately one hour. The route had a downgrade of approximately 1.6%, and braking was accomplished by a combination of standard air brakes and dynamic engine braking. As shown in Figure 2.1, the peak temperature recorded was approximately 110°C. This is very low compared to the estimates of normal freight service conditions, likely due to the very low speed maintained by the ore train (~32.2km/hr prior to braking)[6], [9]. However, the average heating rates at the start of air braking were fairly consistent at ~10°C/min on the first car, both on the level at the top of the hill and on the downgrade segment. The eighth car also shows consistent heating rates, at approximately 3°C/min. This indicates that while the peak temperatures may not be representative, the heat input rate of the brakes was within a range that can be effectively modeled using differential scanning calorimetry.

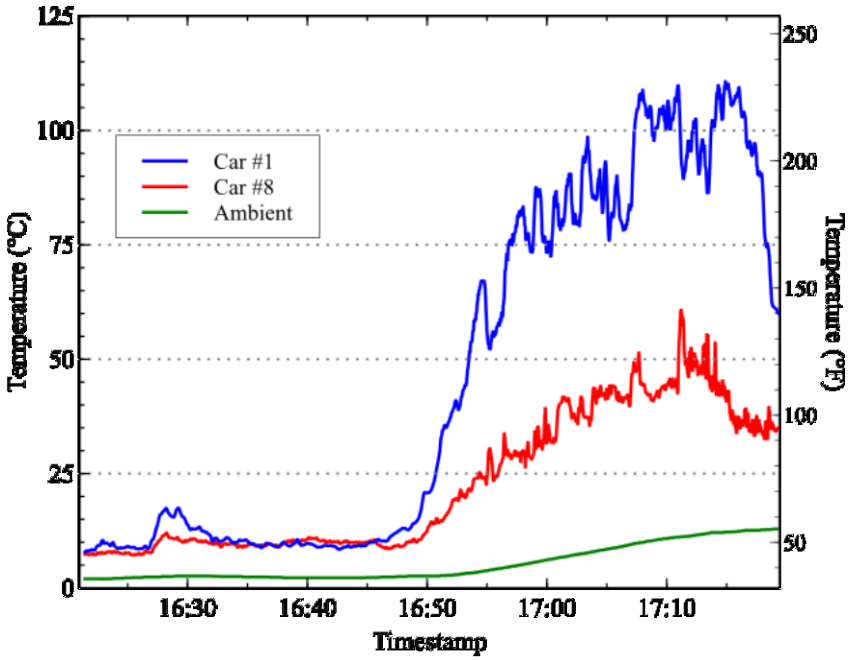

Figure 2.1 Wheel tread temperatures measured on a down-grade run at LS&I. Slight heating at around 16:30 resulted from braking for a slow transition through scales. A 1.6% downgrade starts at approximately 16:45.

2.2 *Peak Service Temperature Limits*

As previously mentioned, there isn't much directly measured wheel temperature data available in the literature. However, analytical models have been used to predict thermal input into rail wheels [2]. Under blended braking (as seen at LS&I), wheel temperatures were predicted to reach 470°C, while air brakes alone might exceed 570°C in extreme conditions and a train intended to use blended braking but experiencing a motor failure could result in tread temperatures in excess of 600°C. It is also important to note that the existing steel wheels are homogenized, quenched around the rim, and then tempered [10]. This is done to produce a beneficial residual stress pattern, but has the side effect of producing tempered martensite, which is isn't thermodynamically stable. As with ADI, exceeding the tempering temperature of the steel will have an in impact on the mechanical properties of the wheel. The wheel will soften, and the internal stresses will shift or be relieved, which may promote fatigue cracking. The tempering temperature reported by Wang and Pilon was 510°C (950°F), which is consistent with the upper range of temperatures predicted by Gordon and Orringer under emergency braking conditions [6].

SECTION 3 CHARACTERIZATION METHODS

3.1 *Metallography*

Microstructural evaluations of all samples were made using an inverted microscope. Samples were mounted in phenolic resin, ground to a 1200 grit finish with silicon carbide abrasive discs (starting at 80 grit), then polished with diamond abrasive to a one micron finish. The final polish was produced using 0.05 micron alumina in a distilled water suspension applied to a nylon polishing cloth. As-polished images were used to characterize the graphite structure of the samples, which has a strong effect on the mechanical properties of the material. High quality ductile iron has a distribution of many round graphite nodules and no flake-like particles, as shown in Figure 3.1.

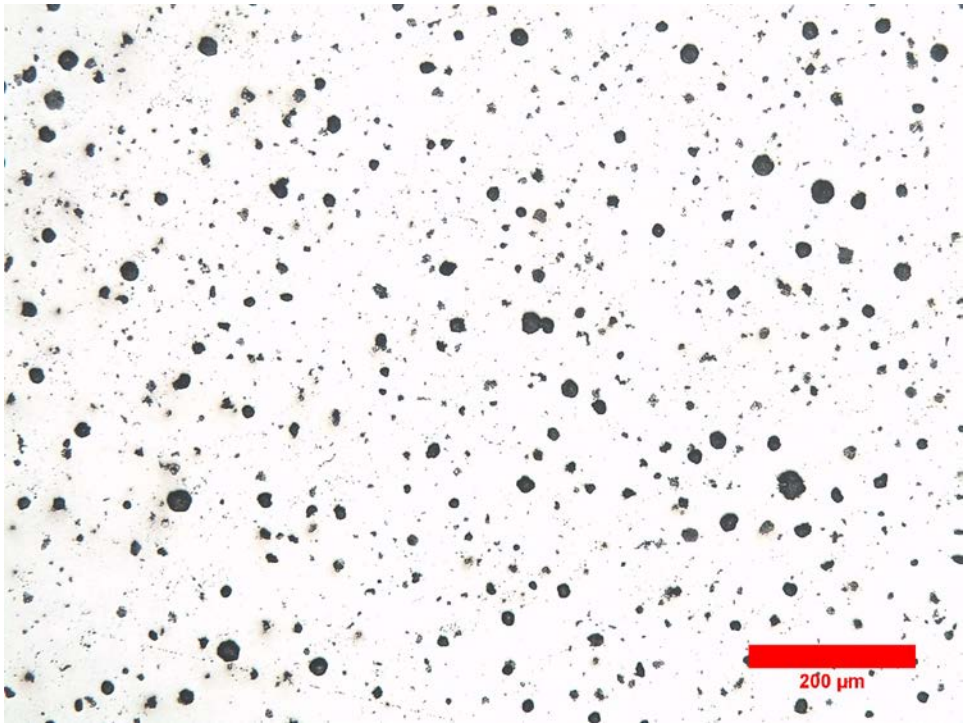

Figure 3.1: Micrograph of polished Grade 1 ADI, showing finely dispersed graphite nodules.

Key metrics for evaluating the quality of the graphite structure in ductile irons are the “nodularity” of the graphite particles and the “nodule count” in the sample. Nodularity is defined as the percentage of graphite particles present that are round enough to be considered nodules (rather than flakes or other morphologies). In order for a particle to qualify as a nodule, it must have a shape factor of at least 0.5, where a perfect circle has a shape factor of 1 and any variation from a circle results in a lower shape factor. The nodule count for a sample is the number of nodules present per square millimeter. A minimum of 500 particles must be analyzed to produce a valid analysis. The graphite analyses for both the commercial ADI and the experimental base alloys produced for this study are presented in Sections 4 and 5, respectively.

3.2 *DSC Analysis*

Samples of each of five grades of commercially produced austempered ductile iron were extracted using wire electrical discharge machining (wire EDM) to minimize heating. This process uses a constant flow of distilled water as a dielectric medium (and coolant) and high voltage to produce an arc

that erodes the sample along the desired path. Five millimeter diameter cylinders were produced, approximately three millimeters tall, to fit in the DSC crucible.

A Netzsch DSC 404 was used to determine the transformation onset temperatures (T_{onset}) at heating rates of 5, 10, and 20 K/min. A nitrogen atmosphere was used for all scans of the as-received ADI. From each grade, a minimum of three scans were performed at each heating rate. The onset temperatures were then plotted to determine the activation energy of the reaction, as described by Kissinger[11].

The activation energy (Q) is calculated by fitting the onset temperature (T_{onset}) at each heating rate (H) to the following, where the gas constant R is required to relate temperature and energy:

$$\frac{d\left(\ln\frac{H}{T_{onset}^2}\right)}{d\left(\frac{1}{T_{onset}}\right)} = -\frac{Q}{R} \tag{3.1}$$

DSC results from the commercially produced grades are presented in section 4.2. Further DSC testing has been delayed due to equipment failures. Once the instrument can be repaired, activation energy determination will be conducted for samples of all test alloys, heat treated to match each of the five initial grades of ADI.

3.3 *Isothermal Transformation*

A temperature-resistant electromagnetic permeability sensor was developed as a means to monitor the austenite decomposition reaction at isothermal conditions in a box furnace. The sensor is designed to supply an alternating electromagnetic field using a coil of high-temperature wire and measure the integrated voltage across a second, concentric coil. A schematic is shown in Figure 3.2. The coupling coefficient between coils is determined by the magnetic permeability of the shared core. When an ADI test bar is used as the core, the decomposition of paramagnetic austenite into ferromagnetic ferrite and cementite will cause a change in the voltage response of the secondary coil.

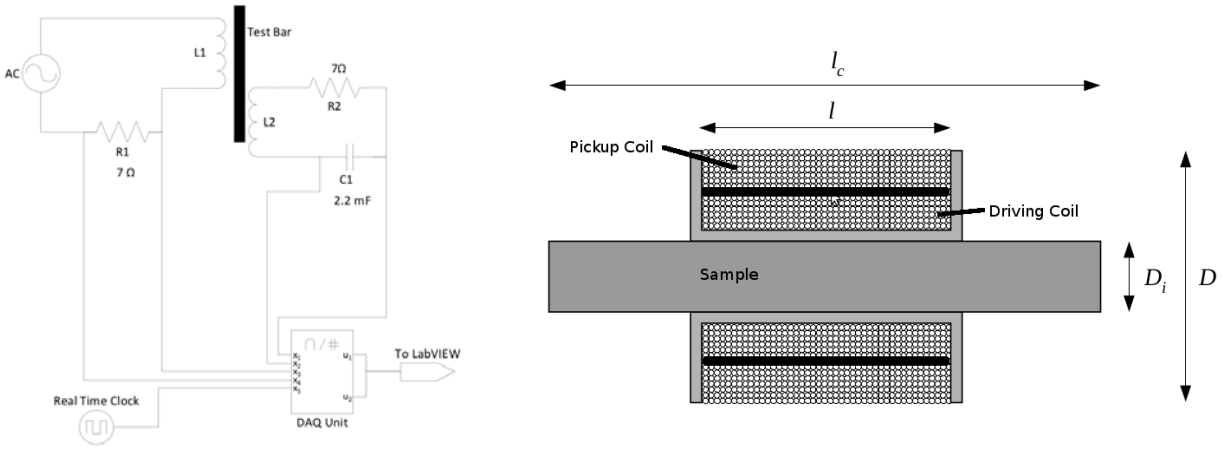

Figure 3.2: Schematics for isothermal transformation sensor. Wiring diagram shown on left, coil construction shown on right.

Differences between grades of ADI have been observed using the sensor at room temperature,

demonstrating that the austenite fraction of the ADI microstructure varies with austempering parameters to an extent that is resolvable with this technique. In order to predict the austenite fraction quantitatively, calibration curves will need to be produced based on x-ray diffraction phase fraction analysis. Once the calibration curves have been generated, further x-ray diffraction work can be minimized in favor of real-time data.

The transition from room temperature to useful furnace temperatures is more complicated than initially expected. The electrical properties of the wire coil change with temperature, and most insulation types are not rated for the temperature range of interest. Fiberglass insulated stranded wire with nickel-clad copper conductors was chosen to best withstand the target temperature range. Calibration of the sensor for elevated temperatures has required the introduction of a reference sensor with an air core, which complicates the measurement and monitoring process.

Development and calibration of the measurement interface is ongoing. Once completed, this system will allow validation of the kinetic model developed from DSC data based on isothermal conditions.

SECTION 4 CHARACTERIZATION OF COMMERCIALLY PRODUCED ADI

4.1 *Metallography and Mechanical Properties*

Table 4.1 provides a summary of the heat treatments and graphite analyses of the initial ADI grades tested. Because heat tinting provides only a qualitative view of matrix microstructure, phase fractions of ferrite, cementite, and austenite are not available at this time. All five grades were produced from a single heat of base iron. The nominal mechanical properties of each grade and the values obtained during this study are given in Table 4.2. Note that not all grades reached the specified properties. However, this may be due to the test bar size used (1/4" gage diameter), rather than the larger sample diameter typically used for certification of castings. This sample geometry was chosen to conserve the available material for testing, but could amplify the effects of minor flaws in the machining or in the microstructure that would have less effect on a larger test bar.

Table 4.1: Heat Treatment Parameters and Graphite Analysis of Commercially Produced ADI

Grade	**Austenitizing Temperature (°C)**	**Austempering Temperature (°C)**	**Austempering Time (min)**	**Graphite Nodularity (% by area)**	**Nodule Count (nodules/mm^2)**	**Particles Analyzed**
1	**896°C**	**382**	**106**	93	591	703
2		**356**	**135**	91	564	654
3		**313**	**182**	90	551	642
4		**282**	**217**	91	606	697
5		**260**	**240**	90	559	662

Table 4.2: ADI specifications and measured mechanical properties.

Grade	ASTM A897 Requirements			Measured Properties		
	UTS (ksi)	Yield (ksi)	% Elongation	UTS (ksi)	Yield (ksi)	% Elongation
1	130	90	9	128	94	12
2	150	110	7	-	-	-
3	175	125	4	171	137	6
4	200	155	2	200	158	4
5	230	185	1	212	163	3

4.2 *DSC Analysis*

The transformation onset temperature was determined for each of nine samples from each grade (three replicates at three heating rates, as noted above). The data was plotted with the natural logarithm of the heating rate on the y axis and the inverse of the onset temperature plotted on the x axis. As shown in Figure 4.1, each grade has a distinct slope, which can be used to determine the activation energy, Q, as shown in Equation 3.1. Note that the data from Grade 3 had a wider scatter, and the fitted slope crosses the line from Grade 4 within the tested range. This result will need to be investigated further to reduce the variability and determine the actual position of the Grade 3 fit.

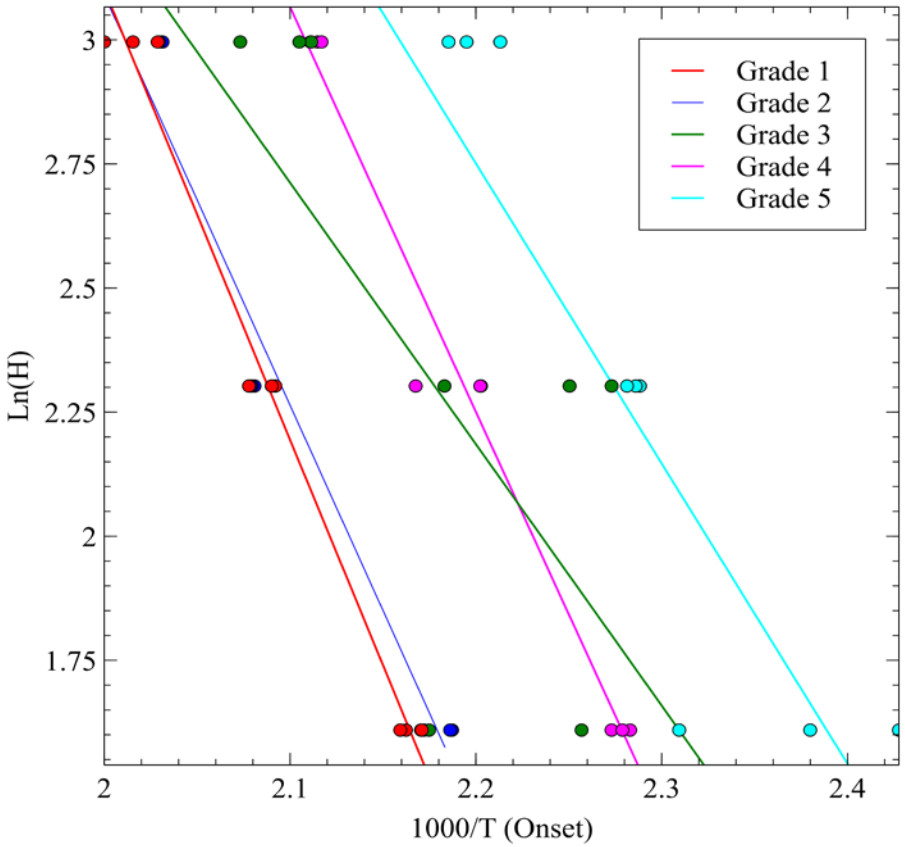

Figure 4.1: Arrhenius Plot of DSC scan results for commercial ADI. Slopes are used to calculate activation energy of transformation.

The slope of each fit can be used to determine the effective activation energy (Q) required to transform each grade of ADI. The results are shown in Figure 4.2, including error bars showing the standard error for the estimate of activation energy. This more clearly shows the need for further analysis of Grade 3. The nominal strengths of each grade are plotted on a secondary axis for reference. The average transformation onset temperatures for each grade and heating condition are given in Table 4.3.

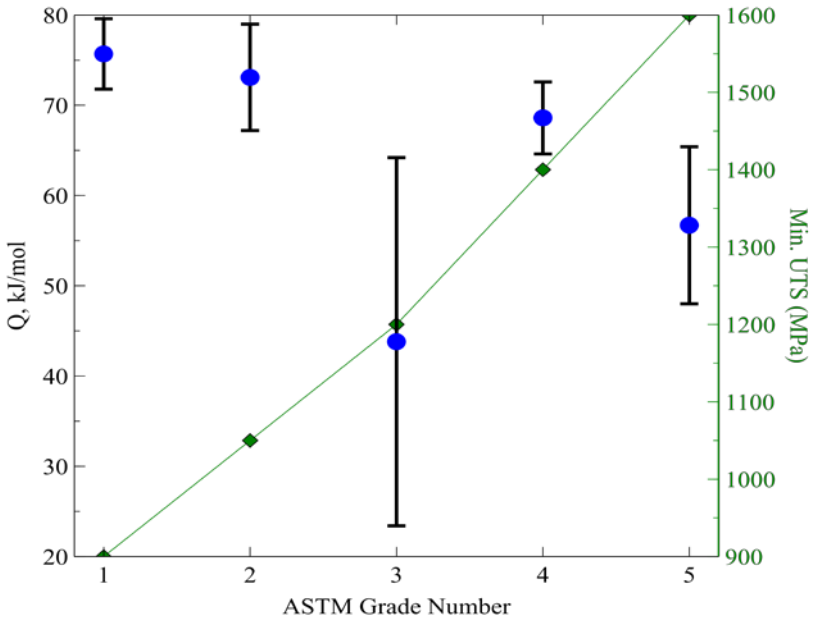

Figure 4.2: Effective activation energies for transformation of commercial ADI grades. Error bars indicate 1 standard error.

Table 4.3: Decomposition onset temperatures for each grade and heating rate.

ADI Grade	Heating Rate, K/min	Onset Temperature, °C
1	5	462
	10	479
	20	496
2	5	458
	10	481
	20	492
3	5	454
	10	447
	20	477
4	5	439
	10	456
	20	473
5	5	422
	10	438
	20	455

SECTION 5 ALLOY DEVELOPMENT

5.1 *Phase Diagrams*

The two primary factors that determine thermodynamic stability for engineering alloys are temperature and composition. Any phase that is theoretically possible within a given alloy system has a range of compositions and temperatures over which it can form, but only the most stable phases are likely to be observed in practice. In some cases, a phase can be observed outside of its stable range because it is faster/easier to form than the stable phase. This is referred to as a metastable phase, and will convert to the stable phase given sufficient time and energy. However, the driving force for this transformation may be quite small, so the metastable phase can exist well beyond practical engineering timescales. By changing alloy composition, it is possible to intentionally reduce this driving force, resulting in thermodynamic stabilization of the metastable phase.

The first method used to screen potential stabilizing additions was thermodynamic phase mapping as a function of alloy addition. This approach was based on the work of Bain regarding steel phase diagrams[12], and shows the way increasing amounts of alloy additions shift the phase field boundaries of the phase diagram. For this study, the expansion of the austenite phase field is the primary concern. In particular, depressing the lower bound of the austenite field decreases the driving force for austenite decomposition. It is also important to note that the carbon solubility of austenite will also change with alloy additions. Figure 5.1 shows that increasing the nickel content of the alloy depresses the lower bound of the austenite field, stabilizing the austenite at lower temperatures (1), but decreases the carbon solubility in austenite (2), which would change the heat treatment parameters required to achieve a comparable ADI grade. A higher austenitizing temperature would be necessary to reach the same carbon saturation, but the resulting ausferrite should be more stable. The effects of the elements screened are summarized in Table 5.1.

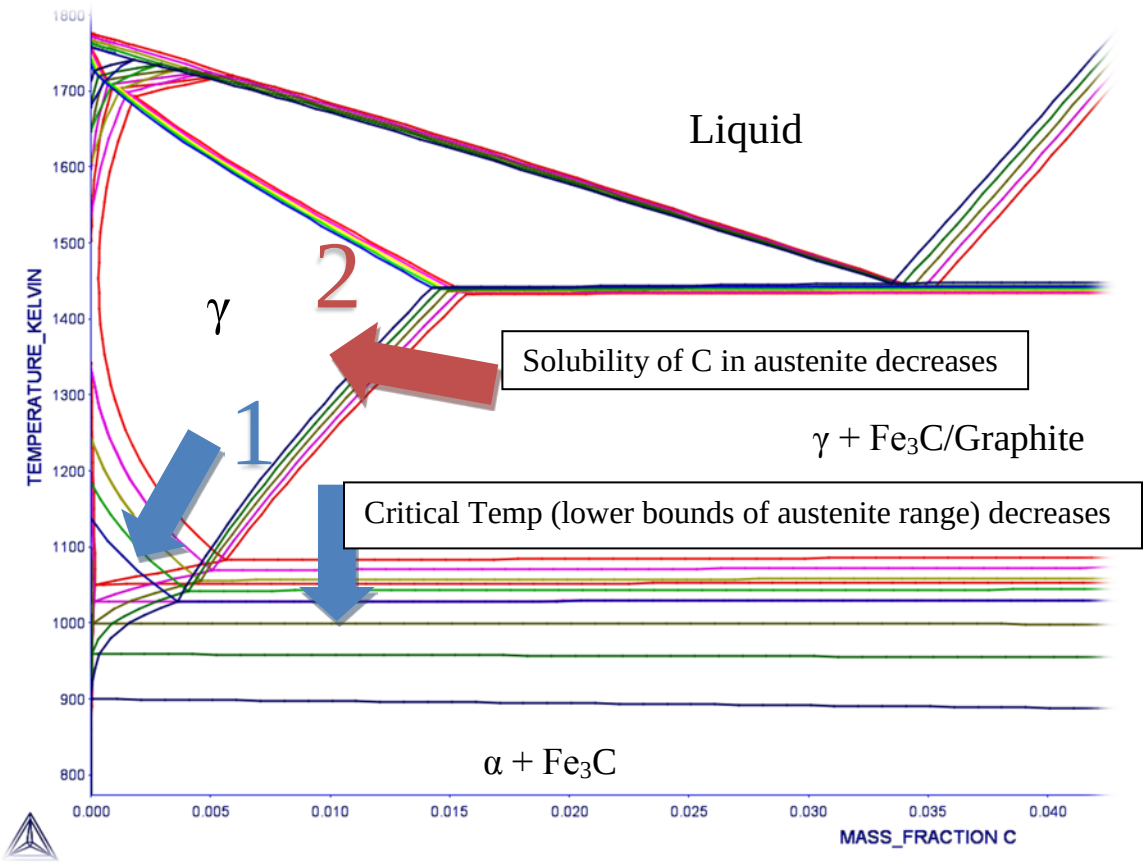

Figure 5.1: Effect of Ni additions on Fe-C phase diagram. Red = 1%, magenta = 2%, yellow = 3%, green = 4%, and blue = 5% Ni.

Based on the phase diagram mapping performed using Thermo-Calc, nickel and cobalt were both identified as austenite stabilizers with potential for use in ADI, as shown in Table 5.1. Nickel is commonly used to increase hardenability for austempering, but usually after the maximum amount of copper is added. Since copper is considered a pearlite promoter and not distinctly an austenite stabilizer (though it does offer some kinetic contribution to that effort), copper was also selected to determine whether or not nickel additions should start at lower copper levels when thermal stability is a concern.

Table 5.1: Thermodynamic effects of increasing alloy additions, 0-5 wt%

Alloying Element	Effect on Phase Diagram		
	Carbon Solubility in Austenite	Critical Temperature	Other Austenite Field Shift
Preferred Effect:	Increase or maintain	Decreases	Expansion
Aluminum	Minimal Effect	Raises	Closes from left
Copper	Reduces	Minimal Effect	Shifts left, splits composition(?)
Molybdenum	Increases	Minimal Effect	Shifts right
Tungsten	Slight Increase	Minimal Effect	Closes from left
Nickel	Decreases	Decreases	Expands, shifting left
Cobalt	Decreases	Decreases	Expands, shifting left

5.2 *Kinetic Stabilization Mechanisms*

In addition to thermodynamic stabilization, which decreases the driving force for austenite transformation, kinetic stabilization has been explored, wherein the rate of the transformation is decreased significantly. This project focused on two main mechanisms to control the transformation rate: decrease the carbon diffusion rate away from the ferrite needles and increase the nucleation energy required for carbides to form.

Any substitutional alloying element will influence carbon diffusion due to the changes in lattice parameter around each substitutional solute atom. A considerable amount of work has been done to characterize the effects of alloying elements on carbon diffusion through austenite in steels[13]–[18]. While this is a useful strategy to note, control of carbon diffusivity alone may not be entirely beneficial. The austempering stage of ADI heat treatment involves the nucleation and growth of ferrite needles into the austenite matrix. This requires carbon to diffuse away from the advancing ferrite boundaries to concentrate in the austenite, so impeding carbon diffusion too much will increase heat treatment time and cost. Ideally, ADI stabilization should focus on increasing the activation energy of carbide nucleation without obstructing the austempering step.

The approach to changing carbide nucleation used in this study was to use a carbide forming element (molybdenum) to compete with cementite (iron carbide) formation. Molybdenum is known to segregate to austenite/ferrite boundaries, where it decreases the activity of the carbon in solution near the boundaries, which makes it less likely to precipitate iron carbides[19]. This also decreases the activity of the molybdenum, which can slow the advancement of the ferrite boundary as well (solute drag effect). Higher activity can be thought of as a less stable state, or taken to mean that there is more energy available for nucleation of a new phase. Because molybdenum diffusion is relatively slow compared to carbon diffusion, molybdenum carbide has a higher effective nucleation activation energy than cementite, so the overall transformation should be obstructed.

5.3 *Alloys Produced*

Based on the thermodynamic data, effects on carbon diffusion, and potential competition effects, five test alloys were produced in the Michigan Tech foundry. The base composition of the commercially-produced ADI was used as a common reference point, and variations with additions of nickel, molybdenum, copper, and cobalt were melted and cast into cylinders. Since the alloys were to be given five different heat treatments, each element was varied independently. This will allow elimination of an alloy from the experiment without confounding other variables, if necessary. Several additional heats would be required in order to combine these studies into a single experimental design and account for interaction effects. This is recommended as an extension of the present work.

The base and experimental compositions produced are given in Table 5.2. Two heats were chosen to evaluate the effects of cobalt concentration, as it was not intentionally included in the base alloy. The commercial and high nickel alloy analyses were performed by outside labs that did not include cobalt in the spectrometer analysis. Metallographic evaluations of the as-cast bars are summarized in Table 5.3.

Table 5.2: Alloy compositions, expressed in weight percent.

Alloy		C	Si	Mg	Ni	Mo	Cu	Co
Commercial	5506	3.56	2.55	0.034	0.02	<0.01	0.48	-
Experimental	H151201A	3.52	2.45	0.017	1.508	0.003	0.460	-
	H160126A	3.479	2.483	0.0396	0.0412	0.0071	0.769	0.0110
	H160126B	3.496	2.533	0.0345	0.0450	0.1974	0.4790	0.0104
	H160127A	3.419	2.565	0.0372	0.0449	0.0074	0.4760	0.4658
	H160127B	3.413	2.562	0.0412	0.0543	0.0091	0.4844	2.359

Table 5.3: Graphite analysis of as-cast experimental alloys.

Alloy	Particles Measured	Nodularity (% by area)	Nodule Count (Nodules/mm^2)
H151201A - High Nickel	891	86	353
H160126A – High Copper	505	94	438
H160126B – High Molybdenum	885	93	398
H160127A – Low Cobalt	502	93	458
H160127B – High Cobalt	839	94	387

After casting the experimental alloys, bars of each composition were heat treated to the Grade 1 specification (Table 4.3) and assessed by DSC to determine the activation energy for decomposition of the ADI material. In this plot, higher values of activation energy indicate improved thermal stability. The effect of Co, a nontraditional ADI alloying element, is particularly noteworthy in the magnitude of the increase in the activation energy and in the stability of the effect over the range of alloying addistion (0.5 to 2.4 wt%).

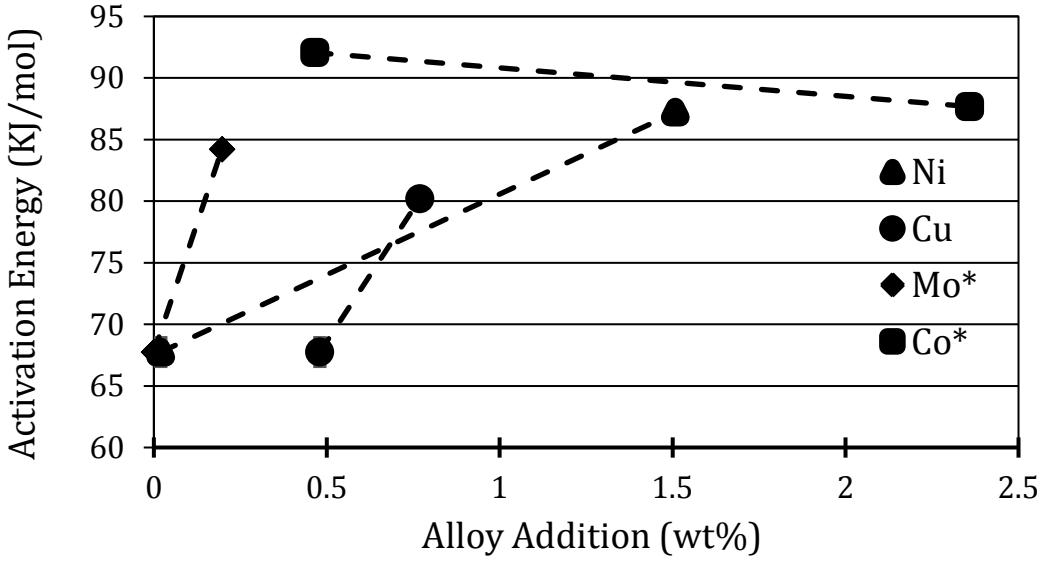

Figure 5.2: Effect of alloying additions of Ni, Cu, Mo, and Cu on the activation energy for decomposition of the ausferrite microconstituent. Mo and Co are not typical ADI alloying elements.

SECTION 6 CONCLUSIONS

Utilization of austempered ductile iron rail wheels offers the opportunity to reduce weight, noise, and cost with improved wear performance. The key challenge is the stability of the ausferrite microstructure (formed during austempering) at elevated service temperatures (e.g. braking). It is considered reasonable for rail wheels to reach ~300°C during normal service, and the ADI grades tested in this study did not begin to transform until they exceeded 400°C, even at a slow heating rate in the least stable grade (Grade 5). Under extreme braking situations, however, steel wheels have been known to exceed 500°C, which is approximately the tempering temperature of the steel wheels. The only ADI samples to approach that temperature prior to transformation were Grades 1 and 2 when rapidly heated. At the heating rates observed at LS&I, those same grades could not exceed 480°C without microstructural changes. The stronger ADI grades would transform even lower, and do not approach the ductility requirements for rail wheels. Stabilization to 500°C seems to be a reasonable target, as it is comparable to the limits of existing wheels.

Utilizing thermodynamic modeling to inform the production of new ADI compositions, cobalt has been identified as potentially improving the thermal stability of the ausferrite matrix. More work is needed to verify alloying effects and quantify the improvement in thermal stability. ADI shows promise, but will require further development before it can be applied to railroad wheels in North American service. Improvements in thermal stability as identified here in conjunction with mechanical property improvements are necessary for a direct conversion to be possible. Further alloy and process development can address both problems, but it remains to be seen whether a suitable balance can be achieved.

SECTION 7 REFERENCES

[1] Keough, "Ductile Iron Data - Section 4," *Ductile Iron Data*, Aug-1998. [Online]. Available: http://www.ductile.org/didata/Section4/4intro.htm. [Accessed: 10-Apr-2015].

[2] K. Madler and D. Bahn, "On the suitability of ADI as an alternative material for (railcar) wheels," *English Translation, GIFA*, 1999.

[3] M. Kuna, M. Springmann, K. Mädler, P. Hübner, and G. Pusch, "Fracture mechanics based design of a railway wheel made of austempered ductile iron," *Engineering Fracture Mechanics*, vol. 72, no. 2, pp. 241–253, Jan. 2005.

[4] ASTM International, "Standard Specification for Austempered Ductile Iron Castings," West Conshohocken, PA, ASTM Standard A897/A897M-15, 2015.

[5] "Wheels, Carbon Steel (M-107/M-208)," in *AAR Manual of Standards and Recommended Practices - Wheels and Axles*, 2011th ed., vol. Section G, Association of American Railroads, 2011, pp. 21–60.

[6] J. E. Gordon and O. Orringer, "INVESTIGATION OF THE EFFECTS OF BRAKING SYSTEM CONFIGURATIONS ON THERMAL INPUT TO COMMUTER CAR WHEELS," 1997.

[7] M. R. Johnson, R. E. Welch, and K. S. Yeung, "ANALYSIS OF THERMAL STRESSES AND RESIDUAL STRESS CHANGES IN RAILROAD WHEELS CAUSED BY SEVERE DRAG BRAKING," Jul. 1975.

[8] D. H. Stone and G. F. Carpenter, "Wheel thermal damage limits," in *Railroad Conference, 1994., Proceedings of the 1994 ASME/IEEE Joint (in Conjunction with Area 1994 Annual Technical Conference)*, 1994, pp. 57–63.

[9] O. Orringer and D. E. Gray, "Thermal cracking in railroad vehicle wheels subjected to high performance stop braking," *Theoretical and Applied Fracture Mechanics*, vol. 23, no. 1, pp. 55–65, Jun. 1995.

[10] K. Wang and R. Pilon, "Investigation of heat treating of railroad wheels and its effect on braking using finite element analysis," in *Proceedings of the International ANSYS Conference, Pittsburgh, PA*, 2002.

[11] H. E. Kissinger, "Variation of Peak Temperature with Heating Rate in Differential Thermal Analysis," *Journal of Research of the National Bureau of Standards*, vol. 57, no. 4, pp. 217–221, 1956.

[12] E. C. Bain, *Functions of the Alloying Elements in Steel*. American Society for Metals, 1939.

[13] A. K. Taheri, T. M. Maccagno, and J. J. Jonas, "Effect of cooling rate after hot rolling and of multistage strain aging on the drawability of low-carbon-steel wire rod," *MMTA*, vol. 26, no. 5, pp. 1183–1193, May 1995.

[14] V. T. L. Buono, B. M. Gonzalez, and M. S. Andrade, "Kinetics of strain aging in drawn pearlitic steels," *Metall and Mat Trans A*, vol. 29, no. 5, pp. 1415–1423, May 1998.

[15] O. K. Rowan and R. D. S. Jr, "Effect of Alloy Composition on Carburizing Performance of Steel," *J. Phase Equilib. Diffus.*, vol. 30, no. 3, pp. 235–241, Apr. 2009.

[16] S.-J. Lee, D. K. Matlock, and C. J. V. Tyne, "An Empirical Model for Carbon Diffusion in Austenite Incorporating Alloying Element Effects," *ISIJ International*, vol. 51, no. 11, pp. 1903–1911, 2011.

[17] R. B. McLellan and C. Ko, "Diffusion of Carbon in Austenite," *Acta Metallurgica*, vol. 36, no. 3, pp. 531–537, 1988.

[18] R. Smoluchowski, "Diffusion Rates of Carbon in Iron-Molybdenum and Iron-Tungsten Alloys," *Physical Review*, vol. 63, no. 11–12, pp. 438–440, 1943.

[19] E. S. Humphreys, H. A. Fletcher, J. D. Hutchins, A. J. Garratt-Reed, W. T. R. Jr, H. I. Aaronson,

G. R. Purdy, and G. D. W. Smith, “Molybdenum accumulation at ferrite: Austenite interfaces during isothermal transformation of an Fe-0.24 pct C-0.93 pct Mo alloy,” *Metall and Mat Trans A*, vol. 35, no. 4, pp. 1223–1235, Apr. 2004.
[20] J. Massone, R. Boeri, and J. Sikora, “Changes in the structure and properties of ADI on exposure to high temperatures,” *International Journal of Cast Metals Research*, vol. 9, pp. 79–82, 1996.
[21] J. Massone, R. Boeri, and J. Sikora, “Decomposition of high-carbon austenite in ADI,” *Transactions of the American Foundrymen’s Society*, vol. 104, pp. 133–137, 1996.
[22] K. L. Hayrynen, B. V. Kovacs, and Keough, J.R., “Determination of Mechanical Properties in Various Ductile Irons After Subjecting Them to Long Term Elevated Temperatures,” Ductile Iron Society, North Olmsted, OH, 28, 1999.
[23] G. Nadkarni, S. Gokhale, and J. Boyd, “Elevated temperature microstructural stability of austempered ductile irons,” *Transactions of the American Foundrymen’s Society*, vol. 104, pp. 985–994, 1996.
[24] M. J. Perez, M. M. Cisneros, E. Valdes, H. Mancha, H. A. Calderon, and R. E. Campos, “Experimental study of the thermal stability of austempered ductile irons,” *Journal of materials engineering and performance*, vol. 11, no. 5, pp. 519–526, 2002.
[25] S. Korichi and R. Priestner, “High-Temperature Decomposition of Austempered Microstructures in Spheroidal Graphite Cast-Iron,” *Materials Science and Technology*, vol. 11, no. 9, pp. 901–907, 1995.
[26] J. Aranzabal, I. Gutierrez, and J. J. Urcola, “Influence of Heat-Treatments on Microstructure of Austempered Ductile Iron,” *Materials Science and Technology*, vol. 10, no. 8, pp. 728–737, 1994.
[27] E. Hepp, V. Hurevich, and W. Schäfer, “Integrated modeling and heat treatment simulation of austempered ductile iron,” *IOP Conference Series: Materials Science and Engineering*, vol. 33, p. 12076, Jul. 2012.
[28] M. J. Perez, M. M. Cisneros, E. Almanza, and S. Haro, “Kinetic Study of the Austempering Reactions in Ductile Irons,” *Journal of materials engineering and performance*, vol. 21, no. 11, pp. 2460–2466, 2012.
[29] S. Gokhale, G. Nadkarni, and S. R. Pundale, “Mechanical Properties of Aged Austempered Ductile Iron,” *Microstructures and mechanical properties of aging materials II*, 1996.
[30] A. Polishetty, B. B. Pan, T. Pasang, and G. Littlefair, “Microstructural Study on Strain Induced Transformation in Austempered Ductile Iron Using Heat Tinting,” 2010, pp. 239–245.
[31] L. Meier, P. Schaaf, S. Cusenza, D. Höche, M. Bamberger, Y. Amran, K. Weiss, M. Hofmann, and H. Hoffmann, “Monitoring Phase Transition Kinetics in Austempered Ductile Iron (ADI),” *Materials Science Forum*, vol. 638–642, pp. 3394–3399, 2010.
[32] Y. J. Park, R. B. Gundlach, and J. F. Janowak, “Monitoring the Bainite Reaction During Austempering of Ductile Iron and High Silicon Cast Steel by Resistivity Measurement,” *AFS Transactions*, vol. 87–97, pp. 411–416, 2003.
[33] A. Trudel, “Service Temperature Sensitivity of ADI Castings.” 1998.
[34] M. Baricco, G. Franzosi, R. Nada, and L. Battezzati, “Thermal effects due to tempering of austenite and martensite in austempered ductile irons,” *Materials Science and Technology*, vol. 15, no. 6, pp. 643–646, 1999.
[35] E. J. Mittemeijer, A. Vangent, and P. J. Vanderschaaf, “Analysis of Transformation Kinetics by Nonisothermal Dilatometry,” *Metallurgical Transactions a-Physical Metallurgy and Materials Science*, vol. 17, no. 8, pp. 1441–1445, 1986.
[36] F. Binczyk, J. Furmanek, and A. Smolinski, “Calorometric Examinations of Austempered Ductile Iron ADI,” *Archives of Foundry Engineering*, vol. 7, no. 4, pp. 5–8, 2007.

[37] R. E. Campos-Cambranis, L. N. Hernandez, M. M. Cisneros-Guerrero, and M. J. Perez-Lopez, “Effect of initial microstructure on the activation energy of second stage during austempering of ductile iron,” *Scripta Materialia*, vol. 38, no. 8, pp. 1281–1287, 1998.
[38] S. Vyazovkin and C. A. Wight, “Isothermal and non-isothermal kinetics of thermally stimulated reactions of solids,” *International Reviews in Physical Chemistry*, vol. 17, no. 3, pp. 407–433, 1998.
[39] C. Yang and S. Létourneau, “Learning to Predict Train Wheel Failures,” in *Proceedings of the Eleventh ACM SIGKDD International Conference on Knowledge Discovery in Data Mining*, New York, NY, USA, 2005, pp. 516–525.
[40] F. Liu, F. Sommer, C. Bos, and E. J. Mittemeijer, “Analysis of solid state phase transformation kinetics: models and recipes,” *International Materials Reviews*, vol. 52, no. 4, pp. 193–212, Jul. 2007.

Appendix A. Conference Paper/Presentation

.

Proceedings of 2014 Joint Rail Conference
JRC2014
April 2-4, 2014, Colorado Springs, Colorado, USA

JRC2014-3781

AUSTEMPERED DUCTILE IRON PERFORMANCE AT RAIL WHEEL OPERATING CONDITIONS

Karl C. Warsinski *
Materials Science and Engineering
Michigan Technological University
Houghton, MI USA
Email: kcwarsin@mtu.edu

Pasi T. Lautala
Civil and Environmental Engineering
Michigan Technological University
Houghton, MI USA
Email: ptlautal@mtu.edu

Paul G. Sanders
Materials Science and Engineering
Michigan Technological University
Houghton, MI USA
Email: sanders@mtu.edu

ABSTRACT

As transportation costs rise, rail stock material improvements are critical to improving efficiency, durability, and performance. Steel wheels have been a consistent part of rail equipment, but it may be time to assess potential other alloys and materials in anticipation of future demands. Strength requirements are steadily increasing with rail car capacity, while weight savings in equipment can reduce fuel costs and/or increase carrying capacity. Herein, the current requirements for railroad wheels are discussed and compared with experimental evaluation of a potential alternative material, austempered ductile iron (ADI).

ADI is an attractive wheel material because of its higher strength-to-weight ratio (as compared to steel) and its wear resistance. ADI castings are also typically cheaper to produce than steel. While ADI can meet or exceed the strength of steel components, it is also comparable in ductility and impact strength, so conversion to ADI does not bring additional risk of brittle fracture, as is commonly the case when achieving higher strengths.

There are challenges with its implementation, however. AAR certification of new materials is costly and time consuming, so adoption is unlikely until there is a very compelling business case. Heat produced during on-tread braking has the potential to damage the heat-treated structure of ADI. The regular exchange of cars across different sections of track and therefore different managing companies requires that new wheel materials be fully backwards compatible, so alterations in design are severely limited. This paper will take initial steps toward assessing the potential of ADI railroad wheels by investigating the performance of ADI at elevated temperatures, and comparing the results to measured and simulated wheel temperatures.

INTRODUCTION AND BACKGROUND

In the last few decades, the allowable axle loads for rail cars in the US have increased significantly. This increases the amount of wear on both wheels and rails, leading to higher maintenance costs. It becomes a tradeoff between fuel efficiency, cargo capacity, and maintenance requirements. If operating loads continue to increase, it may be necessary to convert to alternative materials for rail components to save on equipment weight, decrease wear, or shift wear to the most easily-maintained part of the system.

One promising alternative material is austempered ductile iron (ADI). ADI has been shown to be a promising wheel material for European passenger railroads, demonstrating excellent wear resistance and mechanical properties comparable to steel [1]. ADI can also provide a 10% weight savings, due to the lower density graphite phase distributed within an iron matrix. However, on freight trains, the wheel treads must also serve as part of the braking system, which leads to significant wheel tread temperatures. These temperatures can pose a threat to heat treated material properties. The usefulness of ADI for railroad wheels in the US is constrained by its ability to withstand the most severe braking conditions in service, in addition to the baseline properties required for all rail wheels.

*Address all correspondence to this author.

WHEEL REQUIREMENTS

Material specifications for railroad wheels are established by AAR standard M-107/M-208 [2]. While this standard covers carbon steel wheels, the specifications for Class D wheels provide a meaningful basis for evaluating alternative materials. Several of the mechanical properties required of Class D wheels are given in Table 1. Also shown are the common ranges for these properties in ADI, according to the Ductile Iron Society [3].

TABLE 1. PROPERTIES FOR RAIL WHEELS, AS COMPARED WITH ADI.

	Min. Value	ADI Range
Brinell Hardness	341-415	302-460
UTS (ksi)	157	125-230
Yield Strength (ksi)	110	80-185
% Elongation in 2 in.	14	1-10
Fracture Toughness, MPa$(m)^{1/2}$	38.5	55-70

From this reference data, it is clear that ADI meets most of these specifications already. The biggest area of concern is the ductility measurement (% Elongation), where some development will be necessary.

The property requirements shown are measured at ambient temperatures. However, due to the heat input during braking, rail wheels must maintain sufficient mechanical properties at elevated temperatures. The appealing combination of properties that makes ADI so useful is largely derived from the retention of carbon-stabilized austenite after austempering. This austenite is metastable, meaning that while it will remain under ambient conditions, there is a more stable microstructure that the austenite can decompose into if provided with sufficient activation energy [4–7]. In practice, this means that there is a maximum service temperature for ADI. If an ADI part exceeds this threshold, the microstructure will decompose into ferrite and carbides, changing the "base" properties of the part. An overheated wheel will not recover its previous strength after cooling, as the new microstructure is more thermodynamically stable. For this reason, it is necessary to characterize the decomposition temperature of ADI, and perhaps modify it to shift this decomposition temperature above the working service temperatures expected.

EVALUATION OF ADI STABILITY

In general, ADI has not been recommended for high service temperature applications. There has also been relatively little work done to establish a metric for the upper service temperature limits of ADI. In order to determine whether ADI is stable enough for wheel application in the US, two main data sets are needed. First, the actual wheel tread temperatures faced in service must be determined, or at least approximated. Second, the onset temperature(s) for the decomposition of austenite must be determined. In practice, the austenite decomposition takes a finite amount of time, so very brief exposure to higher temperatures may not result in wheel failure. However, using the nominal onset temperature is a reasonable first approximation service temperature limit.

Wheel Temperature Measurement

The best way to determine the service conditions of rail wheels is to continuously monitor the wheel tread temperature during a fully loaded operating run. However, this data is not normally collected, as it is time consuming and difficult to do so. It is more common to have wayside temperature sensors in areas where extreme conditions are likely or would present a particular hazard.

For the purposes of this study, two infrared sensors were used to monitor the wheel treads of cars #1 and #8 of a short run iron ore train. The sensors were mounted to the leading truck of each car, and a transmitter was mounted at the top of the car to transmit data to a reciever in the locomotive. Temperature readings were captured every two seconds over the course of a one hour trip. After leaving the yard, the train maintained a slow speed through a set of scales, then sped up to ≈32.2 km/hr (20 mph) to continue on to the downhill section of the run. Once on the downgrade, a mix of air braking and dynamic braking was used to control train speed until the end of the run. Ths section of the route has a typical downgrade of 1.6%, and a total drop of 186 meters (610 feet). The results of this test run are shown in Figure 1.

It was found that the mounting brackets used to temporarily mount the sensors to the trucks were not rigid enough to maintain a constant measurement position, leading to considerable noise in the data. In addition, the slow speeds, even on a downgrade run, make this test essentially a proof of method, rather than representative of typical freight operations. Similar testing should be done in more extreme areas (e.g. mountain ranges) in order to characterize the worst case conditions a car might encounter within the interlinked railroad system. Wayside thermal imaging cameras may also be a suitable means of collecting temperature data.

While other sources of direct wheel tread temperature data are still being sought, the issue of wheel temperature profiles has been modeled analytically in the literature, allowing us to evaluate ADI capabilities against a more meaningful data set. In a 1996 DOT study, the temperature ranges expected under various braking configurations were modeled for commuter cars [8]. It was shown that, under extreme conditions, wheel treads may reach temperatures on the order of 538°C (1000°F). Anecdotal

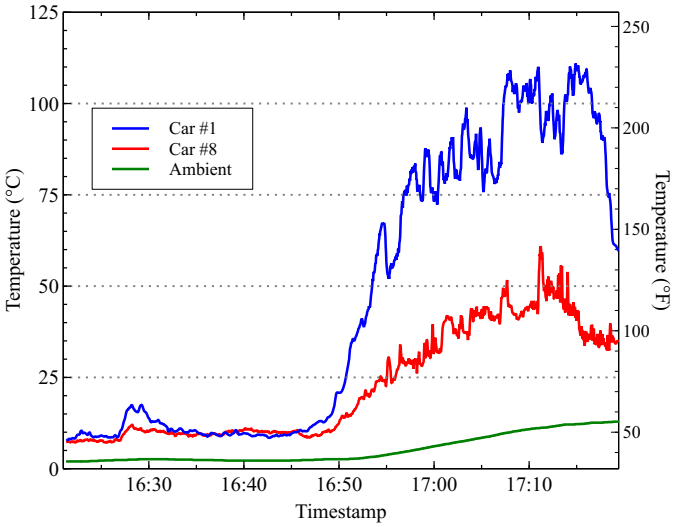

FIGURE 1. WHEEL TREAD TEMPERATURES OVER TIME DURING A DOWNHILL RUN OF AN IRON ORE TRAIN.

information from the freight rail industry suggests similar maximum temperatures.

Transformation Temperatures

A Netzsch DSC 404 differential scanning calorimeter was used to estimate the maximum service temperature of ADI that will not result in austenite decomposition.

Five grades of ADI, produced from a single heat of ductile iron, were procured from a commercial heat treater. The base chemistry is shown in Table 2. The specified properties and heat treatment schedules for each grade are shown in Table 3.

TABLE 2. BASE IRON COMPOSITION, WT%.

C	P	Si	Mn	Cr	Ni	Cu	Fe
3.65	0.027	2.55	0.28	0.07	0.02	0.48	Balance

Cylindrical samples (2mm tall by 5mm diameter) of each grade were produced to fit into the DSC analysis crucibles. Machining was done using a wire EDM to avoid localized destabilization of the microstructure that would skew results with samples of this size. After loading the sample the air was removed from the test furnace using a vacuum pump, and backfilled with nitrogen gas. This was repeated twice, to purge any excess oxygen from the chamber. The test was then conducted with a flowing nitrogen cover gas. Each sample was steadily heated at 10 K/min from 50°C to 650°C.

An example DSC curve is shown in Figure 2. The sharp downward peak represents the transformation of austenite into

TABLE 3. PROPERTIES AND HEAT TREATMENT PARAMETERS FOR ADI GRADES.

	UTS	Yield	Elong.	Austempering	
Gr.	(MPa)	(MPa)	%	Temp. (°C)	Time (min)
1	900	650	9	382	106
2	1050	750	7	356	135
3	1200	850	4	313	182
4	1400	1100	2	282	217
5	1600	1300	1	260	240
All samples austenitized at 896°C for 122 min.					

ferrite and carbide. The curve from each sample was analyzed using the software provided with the instrument to determine the onset temperature for this transformation. This process was then repeated for heating rates of 5 K/min and 20 K/min, with three replicates for each grade and heating rate. Using this data, the onset temperature can be extrapolated for steady-state operations, that is, the minimum temperature at which the transformation will occur at equilibrium [9, 10].

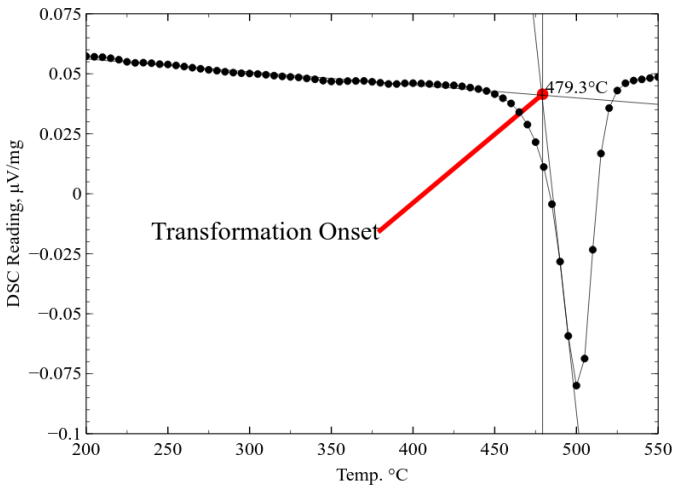

FIGURE 2. TYPICAL DSC CURVE, GRADE 1 ADI.

RESULTS AND CONCLUSIONS

Figure 3 shows the trend in onset temperatures as a function of ADI grade. Additionally, temperature ranges are marked which correspond to the braking configurations modeled in the DOT study described above [8]. The “Blended Braking” condi-

tion is similar to a locomotive's dynamic braking, where a truck-mounted motor is coupled with common air brakes. An "Unpowered Truck" is the typical freight car configuration. The "Motor Failure" regime represents a blended braking truck where the brake assist motor has failed, placing higher than expected braking loads on the air brakes. This would be analogous to a freight car on a long, steep downgrade or one with a stuck brake.

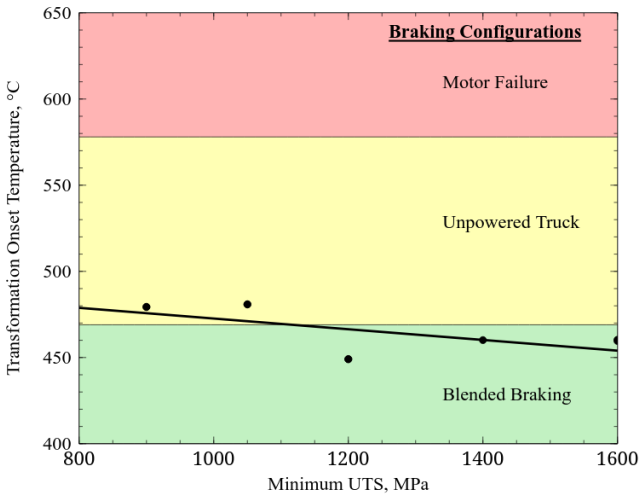

FIGURE 3. ONSET TEMPERATURES BY GRADE, COMPARED WITH TREAD TEMPERATURE MODEL DATA.

It is apparent that the tested ADI grades would be compatible with a blend of direct and dynamic braking. However, the ADI tested in this study would not be suitable for freight car applications, as none of the grades would be able to withstand the emergency case. It is important to note, however, that the kinetics of the austenite decomposition reaction are dependent upon chemistry. Additional studies must be conducted to ascertain which alloying elements or other processing changes will serve to significantly increase the thermal stability of ADI. In addition, it is important that accurate While further development is needed, initial results show that ADI remains a potential material for rail wheel applications.

REFERENCES

[1] Madler, K., and Bahn, D., 2000. "On the suitability of ADI as an alternative material for (railcar) wheels". *Deutsche Bahn, AG-Technical Center, Brandenburg-Kirchmoser, presented in German at the CIATF,* ***99***.

[2] Association of American Railroads, 2011. *Wheels, Carbon Steel Specification M-107/M-208*.

[3] Ductile Iron Group, 1990. *Ductile Iron Data for Design Engineers*. Rio Tinto Iron & Titanium America.

[4] Massone, J., Boeri, R., and Sikora, J., 1996. "Changes in the structure and properties of ADI on exposure to high temperatures". *International Journal of Cast Metals Research,* ***9***, pp. 79–82.

[5] Massone, J., Boeri, R., and Sikora, J., 1996. "Decomposition of high-carbon austenite in ADI". *Transactions of the American Foundrymen's Society,* ***104***, pp. 133–137.

[6] Nadkarni, G., Gokhale, S., and Boyd, J., 1996. "Elevated temperature microstructural stability of austempered ductile irons". *Transactions of the American Foundrymen's Society,* ***104***, pp. 985–994.

[7] Perez, M. J., Cisneros, M. M., Valdes, E., Mancha, H., Calderon, H. A., and Campos, R. E., 2002. "Experimental study of the thermal stability of austempered ductile irons". *Journal of materials engineering and performance,* ***11***(5), pp. 519–526.

[8] Gordon, J., and Orringer, O., 1997. Investigation of the effects of braking system configurations on thermal input to commuter car wheels. Tech. rep., Volpe National Transportation Systems Center.

[9] Kissinger, H., 1956. "Variation of peak temperature with heating rate in differential thermal analysis". *Journal of Research of the National Bureau of Standards,* ***57***(4), pp. 217–221.

[10] Mittemeijer, E. J., Vangent, A., and Vanderschaaf, P. J., 1986. "Analysis of transformation kinetics by nonisothermal dilatometry". *Metallurgical Transactions a-Physical Metallurgy and Materials Science,* ***17***(8), pp. 1441–1445.

Application of Differential Scanning Calorimetry for the Determination of ADI Service Temperature Limits

Karl Warsinski
St. Marys Foundry, Inc. / Michigan Technological University

Background

- DIS Research Project #28
  - Investigated the effect of exposure to elevated temperatures in minimally-alloyed ADI
  - Exposure time = 1000 hours
  - ADI did not maintain mechanical properties for exposures at T > ($T_{austemper}$ – 200°F)
  - Recommended investigation of alloy effects on kinetics of transformation

Project Overview

- Investigate kinetic parameters of ADI degradation
  - 5 heat treatments of same composition
  - Focused on Effective activation energy (E_A) via Kissinger method
- Produce and test alloy variations
  - Can we "move the needle" significantly?
  - 5 Alloys produced
  - HT#1 used for all alloys*

What is DSC?

- Measures temperature differences between a sample and an inert reference during heating

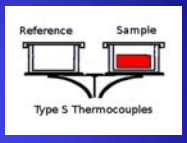

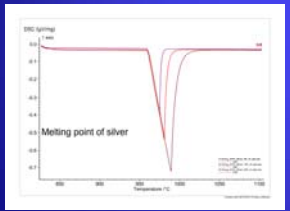

- Deflections/peaks indicate phase changes
- Onset = Start of Transformation
- Peak = Maximum rate

How does this help us?

- Peak position shifts with heating rate when phase changes are thermally activated
- Peak position and heating rate can be used to determine activation energy (E_A)

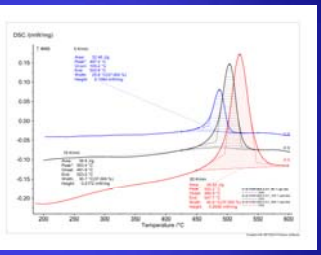

$$d\frac{\ln(\varphi)}{T_p^2} = -\frac{E_A}{R}$$
$$d\left(\frac{1}{T_p}\right)$$

Experimental Alloys

Alloy	C	Si	Ni	Cu	Mo	Co	Mn	P	S	Mg
AP-5506	3.56	2.55	0.02	0.48	<0.01	-	0.28	0.027	0.013	0.034
H151201A	3.52	2.45	1.508	0.46	0.003	-	0.160	0.017	0.005	0.017
H160126A	3.48	2.48	0.041	0.769	0.007	0.011	0.273	0.017	<.001	0.040
H160126B	3.50	2.53	0.045	0.479	0.197	0.010	0.276	0.015	<.001	0.035
H160127A	3.42	2.57	0.045	0.476	0.007	0.466	0.245	0.017	<.001	0.037
H160127B	3.41	2.56	0.054	0.48	0.009	2.359	0.34	0.016	<.001	0.041

Casting Geometry

- AP-5506 – 1" Y-blocks, Received in heat treated condition
  - Samples cut via cooled abrasive saw, wire EDM
- Michigan Tech alloys – ¾"Ø cylinders, 7.5" tall
  - Turned to ½"Ø before heat treating
  - Turned to sub-size tensile samples (1/4" gage, 3/8" grip)
  - DSC samples machined from grip end remainder

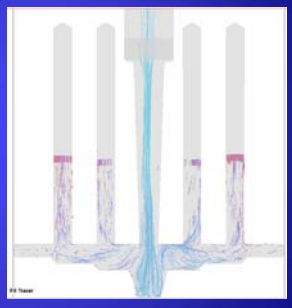

Heat Treatments

	UTS	Yield	Elongation	Austempering	
Grade/HT#	MPa	MPa	%	Temp. (C)	Time (min)
1	900	650	9	382	106
2	1050	750	7	356	135
3	1200	850	4	313	182
4	1400	1100	2	282	217
5	1600	1300	1	260	240

All samples austenitized at 896°C for 122 minutes.

DSC Parameters

- N_2 or Ar atmosphere
- Vacuum and backfill 3x
- Stabilize at 100°C
- Ramp from 100-600°C
  - 5, 10, and 20°/min scans
- Alumina crucibles
- ~170mg Samples
  - (4.5mmØ x 3mm typical)

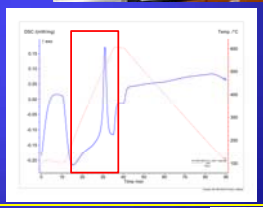

Analysis

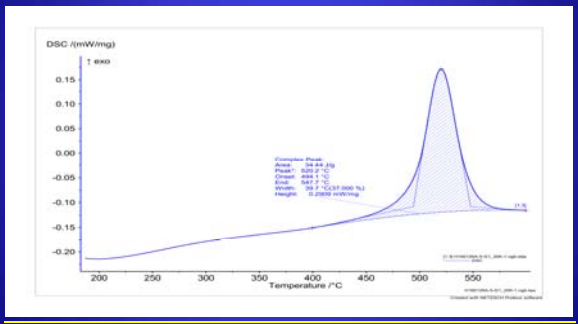

Effect of Treatment Temperature

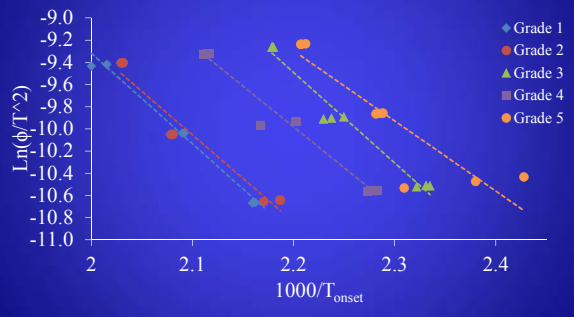

Activation Energy By Treatment Temp.

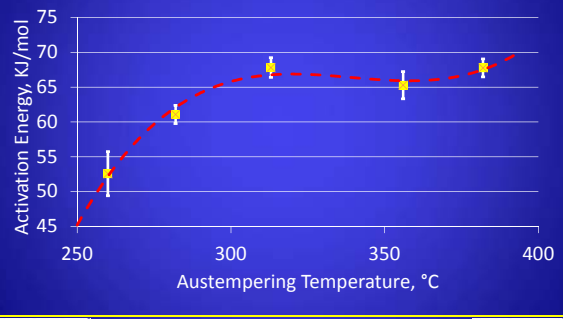

Effect of Alloy Additions

(HT#1)

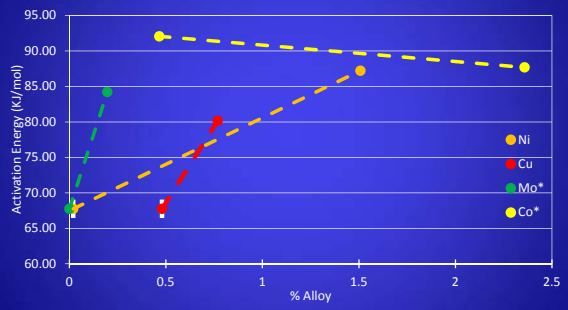

Further Work

Near Term:

- Additional scans to improve regressions
- Test existing alloys with varying heat treatments

Recommended:

- Fill in additional alloy levels
- Develop predictive model for activation energy based on composition and heat treatment

Acknowledgements

This project was supported by the National University Rail (NURail) Center - a US DOT RITA University Transportation Center

Project ID:
NURail2012-MTU-R01

Sample ADI (AP-5506) Provided by Kathy Hayrynen, Applied Process, Inc.

For additional information, please contact:

Karl Warsinski
kwarsinski@stmfoundry.com

Paul Sanders
sanders@mtu.edu